Current Research in Food Science 6 (2023) 100447

Contents lists available at ScienceDirect

Current Research in Food Science

journal homepage: www.sciencedirect.com/journal/current-research-in-food-science

# Apigenin and its octoic acid diester attenuated glycidol-induced autophagic-dependent apoptosis via inhibiting the ERK/JNK/p38 signaling pathways in human umbilical vein endothelial cells (HUVECs)

Yue Zhao [a,b], Qingqing Jiang [a,b], Limin Guo [c], Daming Fan [d], Mingfu Wang [e], Yueliang Zhao [a,b,*]

[a] College of Food Science and Technology, Shanghai Ocean University, Shanghai, 201306, China
[b] Laboratory of Quality and Safety Risk Assessment for Aquatic Products on Storage and Preservation (Shanghai), Ministry of Agriculture, Shanghai, 201306, China
[c] Institute of Agro-Products Storage and Processing, Xinjiang Academy of Agricultural Sciences, Urumqi, 830091, China
[d] School of Food Science and Technology, Jiangnan University, Wuxi, China
[e] Institute for Advanced Study, Shenzhen University, Shenzhen, China

ARTICLE INFO

Handling Editor: Dr. Quancai Sun

*Keywords:*
Glycidol
Autophagy
Apoptosis
Apigenin
Mitogen-activated protein kinase (MAPK)
MAPK signaling Pathway

ABSTRACT

Glycidol is a well-known food contaminant mainly formed in refined edible oils and various thermally processed foods. Here, we studied the toxicity effects and related mechanism of glycidol on Human umbilical vein endothelial cells (HUVECs). Glycidol was found to induce Gap period 2 (G2)/Mitosis (M) phase cell cycle arrest, apoptosis, and autophagy in HUVECs. Inhibition of autophagy by 3-methyladenine (3-MA) attenuated glycidol-induced cell death, suggesting that glycidol-induced apoptosis was autophagy-dependent. Moreover, glycidol treatment induced phosphorylation of extracellular signal-regulated kinase (ERK), c-Jun N-terminal protein kinase (JNK), and p38. Inhibition of ERK, JNK, and p38 phosphorylation by the inhibitors U0126, SP600125, and SB203580 attenuated glycidol-induced autophagy and prevented glycidol-mediated reduction in cell viability, demonstrating that glycidol inhibited HUVECs growth by inducing autophagic-dependent apoptosis through activation of the ERK, JNK and p38 signaling pathways. In addition, apigenin (API) and its octoic acid diester apigenin-7 (API-C8), 4′-O-dioctanoate were found to significantly attenuate glycidol-induced cell growth inhibition by inhibiting the above signaling pathways. Collectively, glycidol induces autophagic-dependent apoptosis via activating the ERK/JNK/p38 signaling pathways in HUVECs and API-C8 could attenuate the toxicity effects.

## 1. Introduction

Glycidol and its esters glycidyl esters (GEs) are well-known food contaminants mainly formed in refined edible oils and thermally processed foods containing salt and fat such as cooked/cured fish or meat, malt-derived products, and bakery products (Jiang et al., 2021; Wang et al., 2021a,b), which implies their frequent exposure by the general public. The epoxide group of glycidol could react with DNA, proteins, and cellular glutathione under physiological systems, and induce many diseases such as kidney toxicity, cardiovascular diseases, and cancers (Bakhiya et al., 2011; Yamada et al., 2010). GEs could be hydrolyzed to form glycidol in the gastrointestinal tract, thus exhibiting the harmful effects (Goh et al., 2021; Liu et al., 2021). Endothelial cells are continuously exposed to and in constant contact with serum circulating substances, making them a target of glycidol (Zhang et al., 2018). Since endothelial cells play a key role in regulating and maintaining vascular health, the dysfunction of endothelial cells has been considered as a key trigger of a number of cardiovascular diseases (Cao et al., 2017; Endemann and Schiffrin, 2004; Little et al., 2021; Wang et al., 2021a,b). Therefore, it is of great significance to study the effect and related mechanism of glycidol on vascular endothelial cells so as to develop effective therapeutic strategies to protect Humans from the toxic effects of glycidol.

Apoptosis, a form of programmed cell death (PCD), is a homeostatic mechanism to maintain cell populations in tissues. Inappropriate apoptosis or increased rate of apoptosis of endothelial cells has been reported to play a deleterious role in the development of common vascular diseases, including atherosclerosis (Dimmeler and Zeiher, 2000; Hao et al., 2021; Hou et al., 2019; Mallat and Tedgui, 2000; Yao et al., 2021). Glycidol has been found to induce apoptosis in Wistar

* Corresponding author. College of Food Science and Technology, Shanghai Ocean University, China.
*E-mail addresses:* yueliang2110@163.com, ylzhao@shou.edu.cn (Y. Zhao).

https://doi.org/10.1016/j.crfs.2023.100447
Received 21 August 2022; Received in revised form 2 December 2022; Accepted 15 January 2023
Available online 16 January 2023

Albino rat brain cells (Sevim et al., 2021). Autophagy is a lysosome-dependent cellular degradation program by which cells utilize lysosomes to degrade their excess or damaged macromolecules and organelles, and the degradation products can be recycled by cells for further use. Basic autophagy is necessary for cellular homeostasis and maintaining the quality of essential components in cells, while excessive or abnormal autophagy can cause cell death and is closely associated with various human diseases including vascular disorders (De Meyer, Grootaert, Michiels, Kurdi, Schrijvers and Martinet, 2015). 3-Monochloropropane diol (3-MCPD) and glycidol co-exposure has been reported to induce autophagic cell death in immortalized rat kidney epithelial cells (NRK-52E cells) (Liu et al., 2021). At present, however, whether glycidol exposure could induce apoptosis and autophagy of vascular endothelial cells and the underlying mechanisms are still unclear.

Apigenin (API) is a natural flavonoid present in various vegetables and fruits with numerous biological activities including cancers, diabetes, inflammation, and cardiovascular diseases (Kashyap et al., 2018). It has been reported to reduce high glucose-increased apoptosis in Human umbilical vein endothelial cells (HUVECs), protect the human brain microvascular endothelial cells (HBMVECs) from oxygen-glucose deprivation/reoxygenation (OGD/R)-induced injury through alleviating apoptosis and autophagy, and attenuated OGD/R induced neuronal injury by its anti-apoptotic and antioxidant properties in rat adrenal pheochromocytoma cells (PC12 cells) (Han et al., 2017; Pang et al., 2018; Qin et al., 2016). Apigenin-7, 4′-O-dioctanoate (API-C8) was an apigenin octoic acid diester identified in fried celeries and was found with higher lipophilicity and cellular antioxidant activity compared to API (Yu et al., 2022; Zhao et al., 2022). Here, we hypothesize that API-C8 could show stronger cell-protective activity than API in HUVECs exposed to glycidol.

In the present study, we investigated the cytotoxic effect of glycidol on HUVECs and the related mechanism. We also further evaluated the protective effect and related mechanism of API and API-C8 on glycidol-induced HUVECs cell damage. Our results could help to develop potential therapeutic strategies to protect Humans from the toxic effect of glycidol.

## 2. Materials and methods

### 2.1. Reagents and antibodies

Glycidol (97%) was purchased from Shanghai Anpel Experimental Technology Co. LTD (Shanghai, China). Trypsin-ethylene diamine tetra acetic acid (trypsin-EDTA) was provided by Gibco Life Technologies (GrandIsland, USA). Primary antibodies against cyclin B1 (12231), p-cdc2 (4539), cdc2 (28439), p-cdc25C (9528), beclin-1 (3738), sequestosome 1 (SQSTM1/p62) (88588), microtubule-associated protein light chain 3 (LC3) I/II (4108), cleaved poly(ADP-ribose) polymerase [PARP] (9541), cleaved caspase-3 (9664), extracellular signal-regulated kinase (ERK) (4695), p38 (8690), c-Jun N-terminal protein kinase (JNK) (9252), p-ERK1/2 (4370), p-p38 (4511), p-JNK (4688), β-actin (4967), and anti-mouse (7076) and anti-rabbit (7074) secondary antibodies conjugated to horseradish peroxidase (HRP) were obtained from Cell Signaling Technology (Berkeley, USA). Hoechst 33342, and cell cycle and apoptosis analysis kit was purchased from Beyotime Corporation (Shanghai, China). 3-Methyladenine (3-MA) was obtained from Selleckchem Chemicals (Houston, USA). SB203580, SP600125 and U0126 were purchased from MedChem Express (NJ, USA). Monodansylcadaverine (MDC) was obtained from Sigma-Aldrich (St. Louis, MO, USA).

### 2.2. Cell culture and cell viability assay

HUVECs obtained from national stem cell resource center (Beijing, China) were cultured in endothelial cell medium (ECM) (ScienCell, USA) containing 5% fetal bovine serum (FBS), 1% endothelial cell growth supplement (ECGS), and 1% antibiotic solution (penicillin/streptomycin) at 37 °C in an incubator under 5% $CO_2$. Cell viability was determined by cell counting kit-8 (CCK-8) assay following the accompanied protocol. In brief, cells ($1 \times 10^4$ cells/well) were cultured in 96-well plates overnight, followed by 24 h incubation with different concentrations of glycidol. After that, the medium was removed and 100 μL of fresh culture medium with CCK-8 solution (10%) was added and followed by incubation at 37 °C for 30 min in the incubator. Absorbance determined at 450 nm using a microplate reader (Biotek, USA) was used to calculate the cell viability (Kamiloglu et al., 2020).

### 2.3. Cell cycle analysis

Cells with a density of $5 \times 10^5$ cells per well were cultured in 6-well plates overnight. After 24 h incubation with various concentration of glycidol, cells were fixed overnight with ethanol (75%) at -20 °C. Then, cells were washed with ice-cold phosphate-buffered saline (PBS) buffer for two times, incubated with 50 μg/mL propidium iodide (PI) containing 100 μg/mL of RNAse-A and 0.1% tritonX-100 for 30 min in the dark, and immediately analyzed by the flow cytometer (BD FACSVerse) (Zhao et al., 2017a,b; Zhao et al., 2019).

### 2.4. Apoptosis assay

Quantitative analysis of apoptosis was carried out using the annexin V-fluorescein isothiocyanate (FITC) apoptosis detection kit I (BD Pharmingen, 556547) according to the manufacturer's protocol. Briefly, cells were cultured overnight in 6-well plates prior to the treatment with glycidol for 24 h. The cells were then collected, washed with PBS and binding buffer, and suspended in binding buffer to obtain a cell concentration of $1 \times 10^6$ per tube. After that, cells were incubated with the annexin V-FITC/PI working solution for 20 min at room temperature in the dark. The stained cells were then diluted by the binding buffer and immediately analyzed by the flow cytometer (BD FACSVerse).

### 2.5. Fluorescent staining

Hoechst 33342 and MDC staining were used for detection of apoptotic chromatin condensation and autophagic vacuoles, respectively (Zhao et al., 2016, 2017a,b; Zhao et al., 2017a,b). Cells ($5 \times 10^5$ cells per well) were seeded in 6-well plates and exposed to 1.4 mM of glycidol for 24 h. Cells were then stained with 0.5 μg/mL of Hoechst 33342 or 1 μg/mL of MDC in the dark for 30 min at 37 °C, washed with PBS for three times, and immediately observed by fluorescence microscopy (Yao et al., 2021).

### 2.6. Western blotting assays

Cells were seeded in 6-well plates. After treatment with different concentrations of glycidol (0, 0.8, 1.2, and 1.4 mM) for 24 h, cells were washed with ice-cold PBS buffer and lysed in radioimmunoprecipitation assay (RIPA) buffer (89900, Thermo Scientific) containing protease inhibitors (Shanghai EpiZyme Biotechnology, GRF101) and phosphatase inhibitors (Shanghai EpiZyme Biotechnology, GRF102). Protein quantification was performed using a bicinchoninic acid (BCA) protein assay kit (Shanghai EpiZyme Biotechnology, ZJ101). Lysate proteins (10 μg) were resolved by sodium dodecyl sulfate polyacrylamide gel electrophoresis (SDS-PAGE), transferred onto polyvinylidene difluoride (PVDF) membranes, and subsequently blocked with Tris-buffered saline, 0.1% Tween 20 (TBST) buffer containing 5% nonfat milk for 1h. The membranes were then incubated with primary antibodies cyclin B1 (1:1000 dilution), p-cdc2 (1:1000 dilution), cdc2 (1:1000 dilution), p-cdc25 (1:1000 dilution), beclin-1 (1:1000 dilution), SQSTM1/P62 (1:1000 dilution), LC3-I/II (1:1000 dilution), cleaved PARP (1:1000 dilution), cleaved caspase-3 (1:1000 dilution), ERK

(1:2000 dilution), p38 (1:1000 dilution), JNK (1:1000 dilution), p-ERK1/2 (1:1000 dilution), p-p38 (1:1000 dilution), p-JNK (1:1000 dilution), β-actin (1:1000 dilution) at 4 °C overnight. After that, the membranes were washed with TBST for three times followed by 1h incubation with HRP-conjugated secondary antibodies (1:2000 dilution) at room temperature. After being washed with TBST three times, the target protein bands were visualized using the enhanced chemiluminescence reagents (ECL) kit and the images were acquired using the ChemiDoc MP imaging system (Bio-Rad). Quantification was performed using ImageJ software (National Institute of Health, Bethesda, MD, United States of America) (Ma et al., 2021).

### 2.7. Statistical analysis

All data were represented as mean ± standard deviation (SD) of three independent experiments. Differences between experimental groups were calculated using Student *t*-test. A *P*-value less than 0.05 was considered statistically significant.

## 3. Results and discussion

### 3.1. Glycidol inhibits cell proliferation and induces $G_2$/M phase cell cycle arrest in HUVECs

Endothelial dysfunction has been considered as a major pathogenic process in atherosclerosis, thrombosis, hypertension, diabetes, and other cardiovascular diseases (Endemann and Schiffrin, 2004; Little et al., 2021). HUVECs are among one of the most popular models used for endothelial cells *in vitro* (Cao et al., 2017). Here the adverse effect of glycidol on endothelial cells was examined in HUVECs. The cell proliferation of HUVECs in response to glycidol treatment was measured by CCK-8 assay. As shown in Fig. 1A, after the exposure of HUVECs to different concentrations (0–1.6 mM) of glycidol for 24 h, glycidol significantly inhibited cell viability in HUVECs dose-dependently with an $IC_{50}$ value of about 1.4 mM. This result was comparable to a study in which glycidol treated for 24 h was found to cause a dose-dependent inhibition of cell viability in the rat kidney epithelial cell (NRK-52E) and the $IC_{50}$ value was about 1.67 mM (Liu et al., 2021; Senyildiz et al., 2017). We next determined the effect of glycidol on cell cycle progression. HUVECs were exposed to various concentrations of glycidol for 24 h and analyzed using flow cytometry. As shown in Fig. 1B, glycidol increased the percentage of cells in the $G_2$/M phase dose-dependently. Further examination of the protein expressions of cell cycle regulators associated with G2 phase arrest showed increased levels of p-cdc2 and p-cdc25C and decreased expression of cyclin B1 and cdc2 (Fig. 1C). These data indicate that glycidol treatment blocked cell growth of HUVECs by inducing $G_2$/M phase cell cycle arrest.

### 3.2. Glycidol induces apoptotic cell death in HUVECs

Hoechst 33342 staining was then performed to examine whether apoptosis was induced in HUVECs in response to glycidol treatment. As shown in Fig. 2A, HUVECs exhibited an appreciable apoptotic response in HUVECs in response to glycidol treatment, as evidenced by the appearance of chromatin-condensed cells. This observation was further confirmed by determining the expression of cleaved caspase-3 and cleaved PARP, two key markers of apoptosis, by Western blotting assay. As shown in Fig. 2B, glycidol treatment for 24 h increased the expression of cleavage PARP and cleavage Caspase-3 in HUVECs dose-dependently indicating apoptosis. A quantitative assessment of apoptosis was then performed by Annexin V-FITC/PI double staining using flow cytometry. Fig. 2C shows that the percentage of apoptotic cells was significantly

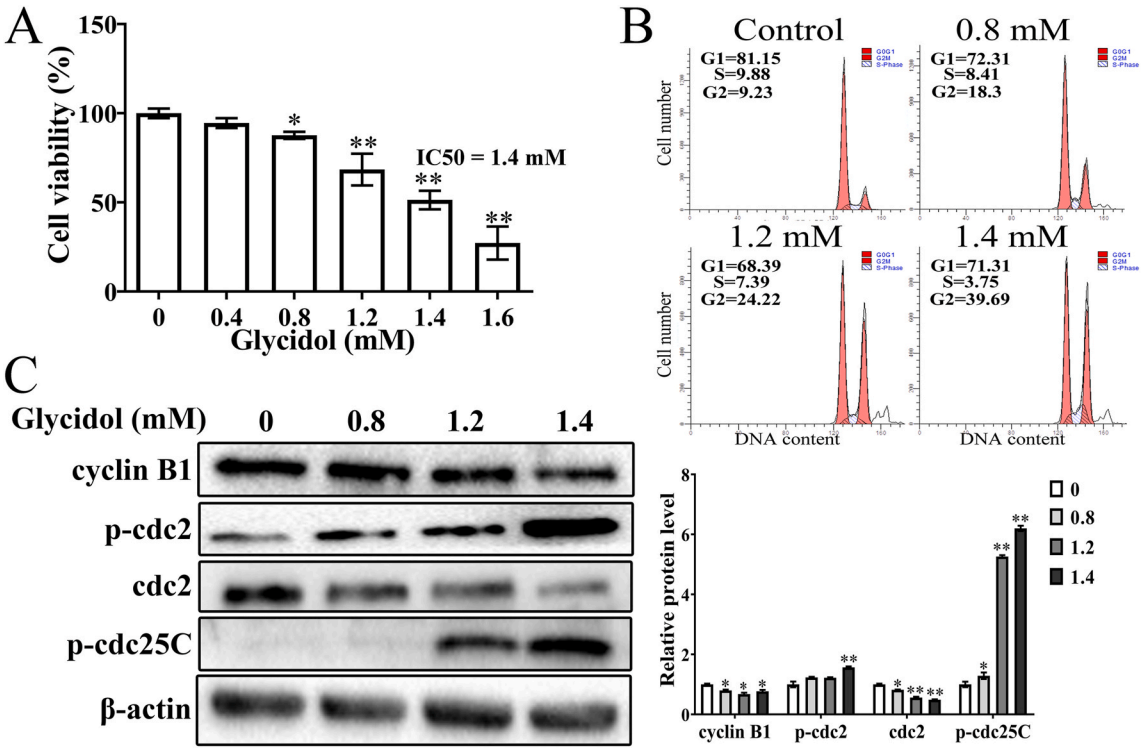


**Fig. 1.** Glycidol inhibits cell proliferation and induces $G_2$/M phase cell cycle arrest in HUVECs. (A) Cytotoxicity of glycidol in HUVECs. Cell viability was measured using the CCK-8 kit after treatment of HUVECs with different concentrations of glycidol for 24 h. Values are mean ± standard deviation, n = 3, $^*P < 0.05$, $^{**}P < 0.01$ Vs the control. (B) HUVECs were treated with glycidol for 24 h, followed by cell cycle distribution assay by flow cytometry. G1, Gap 1; G2, Gap period 2; S, synthesis; M, mitosis. Values are mean ± standard deviation, n = 3, $^*P < 0.05$, $^{**}P < 0.01$ Vs the control. (C) After glycidol treatment at indicated concentrations for 24 h, the effect of glycidol on the indicated protein markers of cell cycle was examined by Western blot. Values are mean ± standard deviation, n = 3, $^*P < 0.05$, $^{**}P < 0.01$ Vs the control.

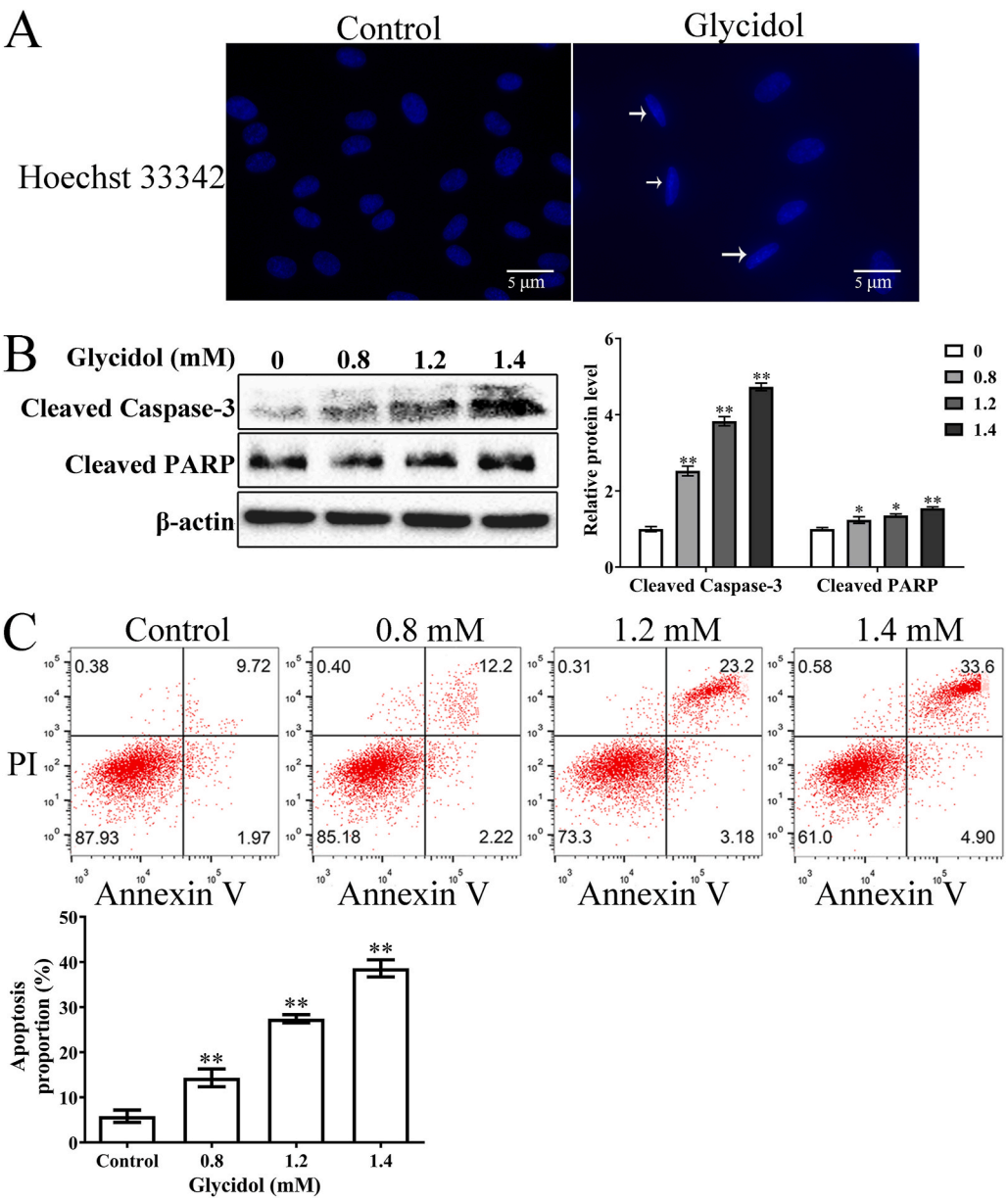


**Fig. 2.** Glycidol induces apoptosis in HUVECs. (A) HUVECs were exposed to 1.4 mM of glycidol for 24 h, subsequently incubated with Hoechst 33342 for 30 min and visualized by fluorescence microscopy. (B) The expression levels of cleaved caspase-3, cleaved PARP and β-actin were determined by Western blot assay after treatment of HUVECs with different concentrations of glycidol for 24 h. Values are mean ± standard deviation, n = 3, $^{*}P < 0.05$, $^{**}P < 0.01$ Vs the control. (C) The percentages of apoptotic cells determined by Annexin V-FITC/PI staining on a flow cytometer after treatment of HUVECs with different concentrations of glycidol for 24 h. Values are mean ± standard deviation, n = 3, $^{*}P < 0.05$, $^{**}P < 0.01$ Vs the control.

increased in glycidol-treated cells compared to vehicle-treated cells. The highest apoptotic rate of 38.5% was observed in cells exposed to 1.4 mM of glycidol for 24 h. Collectively, these data suggested that the reduced cell viability induced by glycidol was associated with apoptotic cell death.

### 3.3. Glycidol-induced apoptosis in HUVECs is autophagy-dependent

Autophagy is likely to be stimulated in response to various endogenous and exogenous stimuli. To determine whether autophagy was involved in glycidol-induced cytotoxicity, some characteristic features of autophagy were examined. MDC was a dye that can accumulate in the mature autophagic vacuoles, such as autophagolysosomes, thus MDC staining was firstly performed for autophagy analysis (Zhao et al., 2017a,b). Fluorescent microscopy clearly showed that the level of MDC-labelled autophagic vacuoles was significantly increased in glycidol-treated cells compared to control (Fig. 3A). LC3, one of the mammalian homologues of yeast Atg8, mainly has two forms, LC3-I and LC3-II. The cytosolic LC3-I is processed into the autophagosome membrane-bound LC3-II in autophagic cells. The amount of LC3-II is correlated with the extent of autophagosome formation. The increased accumulation of LC3-II has been used as an indicator of autophagy induction (Kabeya et al., 2000). Thus, the expression of LC3-II was then examined by Western blotting assay. Fig. 3B showed that glycidol treatment significantly increased the level of LC3-II in a dose-dependent manner in HUVECs. Importantly, glycidol treatment significantly down-regulated the expression level of SQSTM1/p62, a typical autophagy substrate (Fig. 3B). Glycidol treatment also enhanced the expression beclin-1, a gene that was crucial for the autophagy execution, in a dose-dependent manner (Lee et al., 2021). These results strongly support that the effect of glycidol treatment on HUVECs includes induction of autophagy.

After demonstrating that apoptosis and autophagy were induced in HUVECs following glycidol treatment, we next studied the relationship of these two events. 3-Methyladenine (3-MA) has been widely used as inhibitors of autophagy both *in vitro* and *in vivo* (Chicote et al., 2020). To determine the role of autophagy in glycidol-induced apoptosis, the effect of 3-MA on glycidol-induced cell death in HUVECs was evaluated. As expected, 3-MA significantly inhibited autophagy, as evidenced by the reduced accumulation of LC3-II and increased accumulation of p62 in

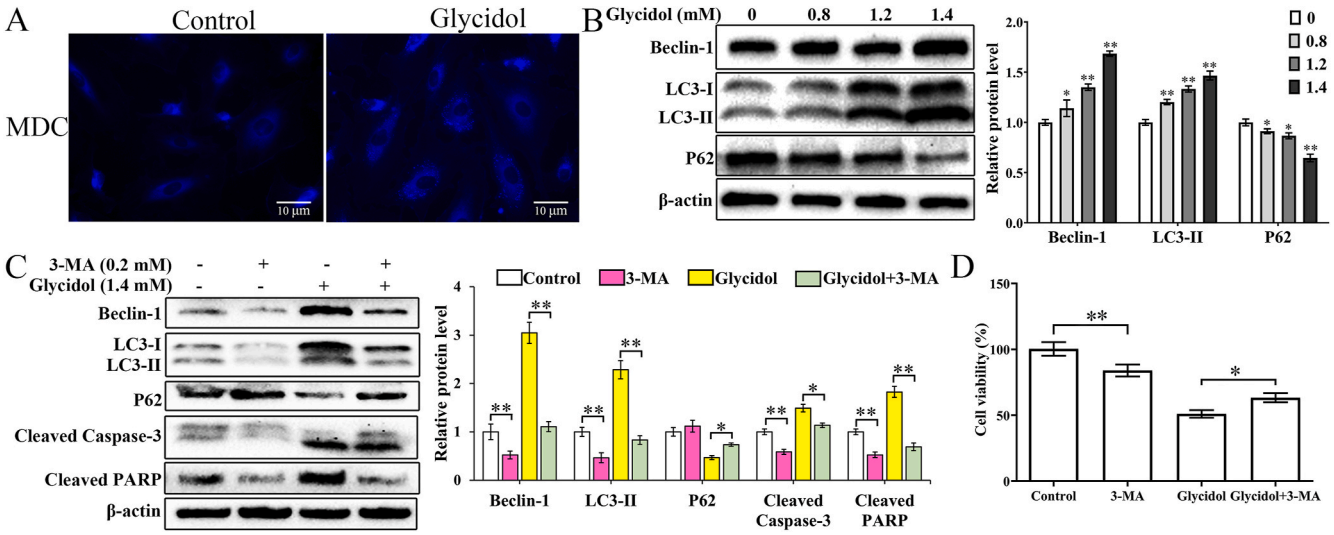


**Fig. 3.** Glycidol induced autophagy and inhibition of autophagy attenuated glycidol-induced apoptotic cell death. (A) HUVECs were exposed to 1.4 mM of glycidol for 24 h, stained with MDC for 30 min and visualized by fluorescence microscopy. (B) The expression of beclin-1, p62, LC3-II, and β-actin were determined by Western blot assay after treatment of HUVECs with different concentrations of glycidol for 24 h. Values are mean ± standard deviation, n = 3, $^{*}P < 0.05$, $^{**}P < 0.01$ Vs the control. (C) The expression of beclin-1, LC3-II, p62, cleaved caspase-3 and cleaved PARP were determined by Western blot assay after treatment of HUVECs with 1.4 mM glycidol in the presence or absence of 0.2 mM of 3-MA for 24 h. Values are mean ± standard deviation, n = 3, *, ** between samples indicate statistically significant differences, $^{*}P < 0.05$, $^{**}P < 0.01$. (D) Cell viability was measured after treatment of HUVECs with 1.4 mM glycidol in the presence or absence of 0.2 mM of 3-MA for 24 h. Values are mean ± standard deviation, n = 3, *, ** between samples indicate statistically significant differences, $^{*}P < 0.05$, $^{**}P < 0.01$.

HUVECs (Fig. 3C). Importantly, when HUVECs were co-treated with glycidol and 3-MA, the expression of cleaved caspase-3 and cleaved PARP were markedly decreased in comparison with cells treated with glycidol alone (Fig. 3C), and 3-MA and glycidol co-treatment significantly improved cell survival compared to glycidol treatment alone (Fig. 3D). Collectively, these findings suggested that glycidol-induced apoptotic cell death was, at least in part, dependent on glycidol-induced autophagy in HUVECs.

### 3.4. Glycidol induces autophagy and apoptosis through activating the ERK/JNK/p38 signaling pathways in HUVECs

The mitogen-activated protein kinase (MAPK) cascades are key intracellular signal transduction pathways that are involved in the regulation of a large number of fundamental cellular processes including growth, proliferation, autophagy, and apoptosis. There are three major groups of mammalian MAPK: the extracellular signal-regulating kinase (ERK), c-Jun N-terminal protein kinase (JNK), and p38 (Plotnikov et al., 2011; Sui et al., 2014). We next evaluated whether MAPK activation was involved in glycidol-induced apoptosis and autophagy. Cell viability of HUVECs exposed to glycidol for 24 h in the presence or absence of various MAPK inhibitors including the ERK inhibitor U0126, the JNK inhibitor SP600125, and the p38 inhibitor SB203580 were measured. All of the three inhibitors were found to partially alleviate glycidol-induced reduction in cell viability (Fig. 4A), indicating that glycidol may inhibit cell proliferation through activating the ERK/JNK/p38 MAPK signaling pathways. We then determined whether glycidol treatment indeed induced ERK, JNK and p38 activation in HUVECs by Western blot assay. As expected, glycidol increased the level of phosphorylated ERK, phosphorylated JNK, and phosphorylated p38 (Fig. 4B), further demonstrating the involvement of ERK, JNK and p38-associated signaling pathways in glycidol-induced cell growth inhibition of HUVECs. We then assessed whether ERK, JNK and p38 activation are required for glycidol-induced autophagy and apoptosis. U0126, SP600125, and SB203580 significantly attenuated the expression levels of beclin-1 and LC3-II, but restored the expression levels of p62 in glycidol-treated HUVECs (Fig. 4C–4E), indicating the involvement of ERK, JNK and p38 activation in glycidol-induced autophagy. Moreover, the three inhibitors significantly attenuated the levels of cleaved caspase-3 and cleaved PARP in glycidol-treated HUVECs (Fig. 4C–4E), suggesting that the activation of ERK, JNK and p38 were involved in glycidol-induced apoptosis. Collectively, these findings suggested that glycidol-induced apoptosis and autophagy were, at least in part, through activating the ERK/JNK/p38 MAPK signaling pathways.

### 3.5. API and API-C8 inhibit glycidol-induced autophagy and apoptosis via inhibiting the ERK/JNK/p38 signaling pathways in HUVECs

To investigate the protective potential of apigenin (API) and its octoic acid diester apigenin-7, 4′-O-dioctanoate (API-C8) on glycidol induced cytotoxicity, their cytotoxicity was firstly evaluated by the CCK-8 assay. As shown in Fig. 5A, 0 to 10 μM of API and 0 to 50 μM of API-C8 treatment for 24 h did not show any cytotoxicity toward the HUVEC. 0 to 10 μM of API was also found non-toxic to HUVEC in another study (Zhou et al., 2019). 10 μM of API and API-C8 was chosen for further evaluations as they had no significant toxicity on HUVECs at this concentration. 10 μM of API improved cell survival by 18.3% and 10 μM of API-C8 improved cell survival by 40.4% in response to glycidol treatment, that is, API-C8 exhibited stronger cell protective effect than API (Fig. 5B). In agreement with our findings, API was also found to inhibit high glucose-increased apoptotic cell death in HUVECs (Qin et al., 2016). Importantly, co-treatment with glycidol and API or API-C8 significantly reduced the expression of cleaved caspase-3 and cleaved PARP in HUVECs compared to cells treated with glycidol alone (Fig. 5C), indicating that API and API-C8 inhibited glycidol-induced apoptosis. API or API-C8 attenuated the expression levels of beclin-1 and LC3-II but restored the expression levels of p62 in glycidol-treated HUVECs (Fig. 5D), suggesting that API and API-C8 inhibited glycidol-induced autophagy. Moreover, API and API-C8 significantly attenuated glycidol-induced ERK, JNK and p38 activation as evidenced by the down-regulated expression of p-ERK, p-JNK and p-p38 (Fig. 5E). Collectively, our data indicated that API and API-C8 inhibited glycidol-induced autophagy and apoptotic cell death via inhibiting the ERK/JNK/p38 MAPK signaling pathways in HUVECs. Apigenin was also found to inhibit inflammatory responses in NIH-3T3 cells and HUVECs by inhibiting JNK activation (Funakoshi-Tago et al., 2011; Wang et al.,

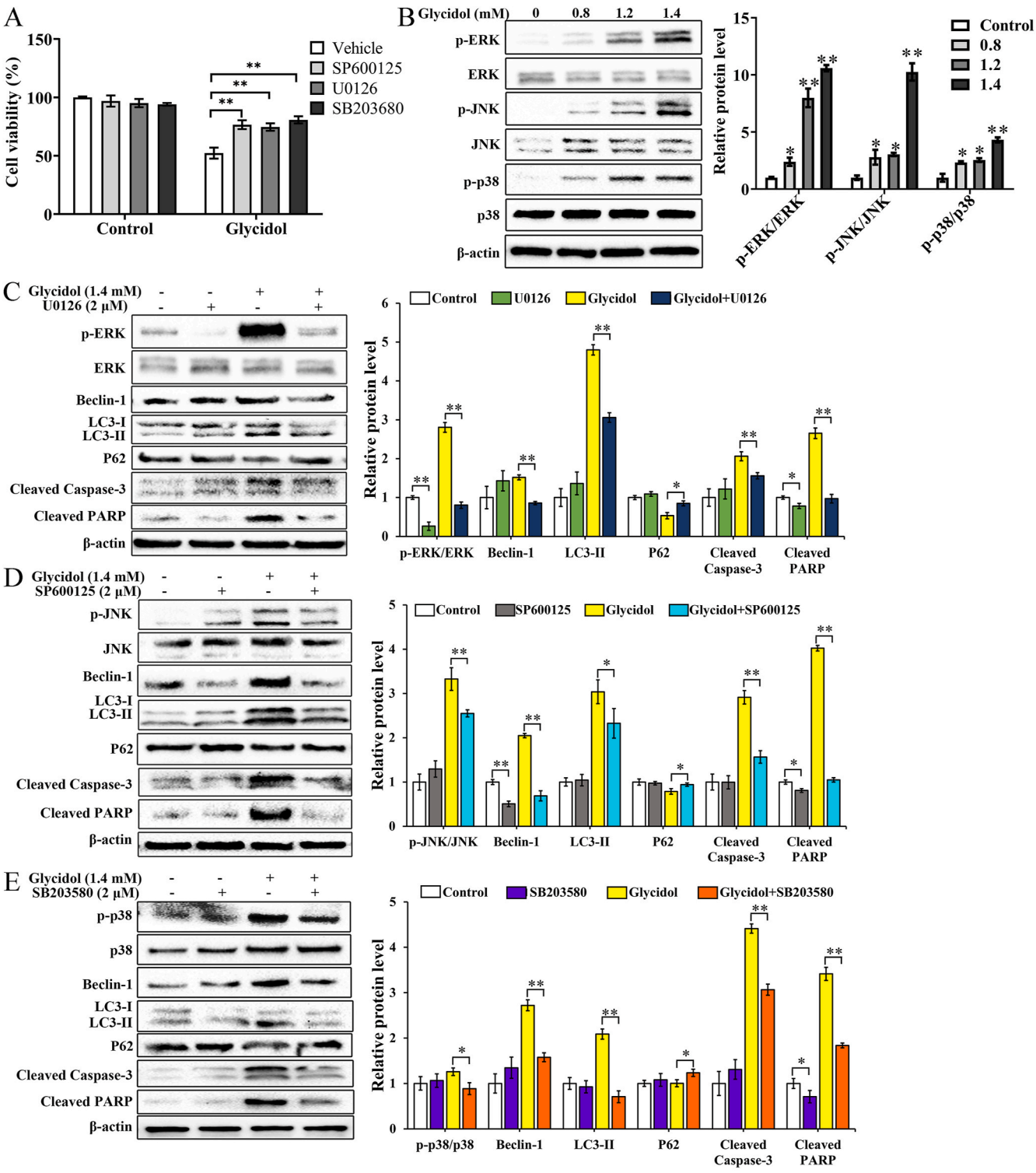


**Fig. 4.** Glycidol induces autophagy and apoptosis through activating the ERK/JNK/p38 signaling pathways in HUVECs. (A) Cell viability of HUVECs treated with 1.4 mM of glycidol in the presence or absence of 2 μM of U0126, SP600125 or SB203580 for 24 h. Values are mean ± standard deviation, n = 3, *, ** between samples indicate statistically significant differences, $^{*}P < 0.05$, $^{**}P < 0.01$. (B) The expression levels of p-ERK, ERK, p-JNK, JNK, p-p38, p38, and β-actin were determined by Western blot assay after treatment of HUVECs with different concentrations of glycidol for 24 h. The expression levels of p-ERK, ERK, p-JNK, JNK, p-p38, p38, beclin-1, LC3-II, p62, cleaved caspase-3, and cleaved PARP were determined by Western blot assay after treatment of HUVECs with 1.4 mM glycidol in the presence or absence of 2 μM of (C) U0126, (D) SP600125, and (E) SB203580 for 24 h. Values are mean ± standard deviation, n = 3, *, ** between samples indicate statistically significant differences, $^{*}P < 0.05$, $^{**}P < 0.01$.

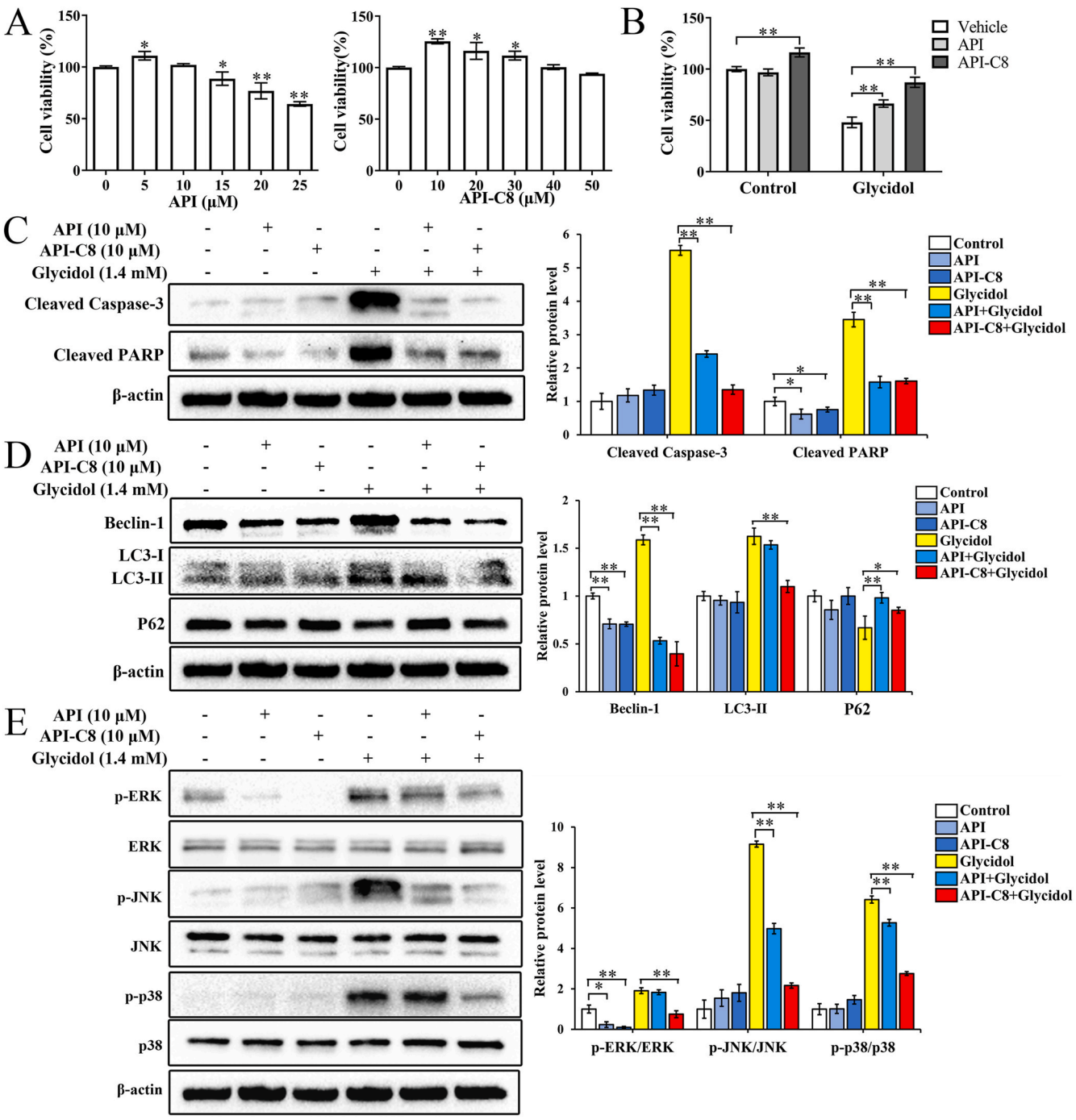


**Fig. 5.** API and API-C8 inhibit glycidol-induced autophagy and apoptosis via inhibiting the ERK/JNK/p38 signaling pathways in HUVECs. (A) HUVECs were incubated with different concentrations of API or API-C8 for 24 h, followed by cell viability assay using a CCK-8 kit. Values are mean ± standard deviation, n = 3, $^{*}P < 0.05$, $^{**}P < 0.01$ Vs the control. (B) HUVECs were incubated with 1.4 mM glycidol in the presence or absence of 10 μM of API or API-C8 for 24 h, followed by cell viability assay using a CCK-8 kit, detection of (C) cleaved caspase-3 and cleaved PARP, (D) beclin-1, LC3-II and p62 and (E) p-ERK, ERK, p-JNK, JNK, p-p38, p38, and β-actin by Western blot assay. Values are mean ± standard deviation, n = 3, *, ** between samples indicate statistically significant differences, $^{*}P < 0.05$, $^{**}P < 0.01$.

2012).

## 4. Conclusions

In summary, glycidol exhibited HUVECs cytotoxicity by inducing $G_2$/M phase cell cycle arrest and autophagy-dependent apoptosis. Activation of the ERK/JNK/p38 signaling pathways may account for the adverse effects of glycidol on HUVECs. Moreover, API and API-C8 strongly relieved the cytotoxic effect of glycidol through inhibiting the ERK/JNK/p38 signaling pathways. Our results could help to develop potential therapeutic strategies to protect Humans from the toxic effect of glycidol.

## CRediT authorship contribution statement

**Yue Zhao:** Investigation, Methodology, Writing – original draft. **Qingqing Jiang:** Methodology. **Limin Guo:** Methodology. **Daming Fan:** Writing – review & editing. **Mingfu Wang:** Supervision, Writing – review & editing, Funding acquisition. **Yueliang Zhao:** Methodology, Supervision, Writing – review & editing, Funding acquisition.

## Declaration of competing interest

The authors declare that they have no known competing financial interests or personal relationships that could have appeared to influence the work reported in this paper.

## Acknowledgements

This work was financially supported by the "National Natural Science Foundation of China (31901807 & 31871901)" and "Shanghai Young Oriental Scholar Program (QD2019033)".

## References

Bakhiya, N., Abraham, K., Gürtler, R., Appel, K.E., Lampen, A., 2011. Toxicological assessment of 3-chloropropane-1, 2-diol and glycidol fatty acid esters in food. Mol. Nutr. Food Res. 55 (4), 509–521.

Cao, Y., Gong, Y., Liu, L., Zhou, Y., Fang, X., Zhang, C., Li, Y., Li, J., 2017. The use of human umbilical vein endothelial cells (HUVECs) as an *in vitro* model to assess the toxicity of nanoparticles to endothelium: a review. J. Appl. Toxicol. 37 (12), 1359–1369.

Chicote, J., Yuste, V.J., Boix, J., Ribas, J., 2020. Cell death triggered by the autophagy inhibitory drug 3-methyladenine in growing conditions proceeds with DNA damage. Front. Pharmacol. 1632.

De Meyer, G.R., Grootaert, M.O., Michiels, C.F., Kurdi, A., Schrijvers, D.M., Martinet, W., 2015. Autophagy in vascular disease. Circ. Res. 116 (3), 468–479.

Dimmeler, S., Zeiher, A.M., 2000. Endothelial cell apoptosis in angiogenesis and vessel regression. Circ. Res. 87 (6), 434–439.

Endemann, D.H., Schiffrin, E.L., 2004. Endothelial dysfunction. J. Am. Soc. Nephrol. 15 (8), 1983–1992.

Funakoshi-Tago, M., Nakamura, K., Tago, K., Mashino, T., Kasahara, T., 2011. Anti-inflammatory activity of structurally related flavonoids, Apigenin, Luteolin and Fisetin. Int. Immunopharm. 11 (9), 1150–1159.

Goh, K.M., Wong, Y.H., Tan, C.P., Nyam, K.L., 2021. A summary of 2-, 3-MCPD esters and glycidyl ester occurrence during frying and baking processes. Current Research in Food Science 4, 460–469.

Han, Y., Zhang, T., Su, J., Zhao, Y., Wang, C., Li, X., 2017. Apigenin attenuates oxidative stress and neuronal apoptosis in early brain injury following subarachnoid hemorrhage. J. Clin. Neurosci. 40, 157–162.

Hao, R., Ge, J., Li, M., Song, X., Jiang, Y., Li, F., Sun-Waterhouse, D., Li, D., 2021. Caffeic acid phenethyl ester mitigates cadmium-induced damage via the Hsa_circ_0010039/miR-661/Caspase9 axis–mediated apoptosis. Food Frontiers 2 (4), 537–546.

Hou, K., Yu, Q., Hu, X., Ding, X., Hong, J., Chen, Y., Xie, J., Nie, S., Xie, M., 2019. Protective effect of *Ganoderma atrum* polysaccharide on acrolein-induced macrophage injury via autophagy-dependent apoptosis pathway. Food Chem. Toxicol. 133, 110757.

Jiang, L., Jing, Z., Yibaina, W., Yan, S., Lili, X., Yanxu, Z., Ling, Y., Pingping, Z., Haixia, S., Lei, Z., 2021. Dietary exposure to fatty acid esters of monochloropropanediols and glycidol of 2-to 3-year-old children attending nursery schools from two areas in China using the duplicate-diet collection method. Food Addit. Contam. 38 (1), 70–80.

Kabeya, Y., Mizushima, N., Ueno, T., Yamamoto, A., Kirisako, T., Noda, T., Kominami, E., Ohsumi, Y., Yoshimori, T., 2000. LC3, a mammalian homologue of yeast Apg8p, is localized in autophagosome membranes after processing. EMBO J. 19 (21), 5720–5728.

Kamiloglu, S., Sari, G., Ozdal, T., Capanoglu, E., 2020. Guidelines for cell viability assays. Food Frontiers 1 (3), 332–349.

Kashyap, D., Sharma, A., Tuli, H.S., Sak, K., Garg, V.K., Buttar, H.S., Setaer, W., Sethi, G., 2018. Apigenin: a natural bioactive flavone-type molecule with promising therapeutic function. J. Funct.Foods 48, 457–471.

Lee, X.C., Werner, E., Falasca, M., 2021. Molecular mechanism of autophagy and its regulation by cannabinoids in cancer. Cancers 13 (6), 1211.

Little, P.J., Askew, C.D., Xu, S., Kamato, D., 2021. Endothelial dysfunction and cardiovascular disease: history and analysis of the clinical utility of the relationship. Biomedicines 9 (6), 699.

Liu, P.W., Li, C.I., Huang, K.C., Liu, C.S., Chen, H.L., Lee, C.C., Chiou, Y.Y., Chen, R.J., 2021. 3-MCPD and glycidol coexposure induces systemic toxicity and synergistic nephrotoxicity via NLRP3 inflammasome activation, necroptosis, and autophagic cell death. J. Hazard Mater. 405, 124241.

Ma, Y.L., Yang, Y., Thakur, K., Cespedes-Acuña, C.L., Zhang, J.G., Wei, Z.J., 2021. Evaluation of spatial memory and anti-fatigue function of long-term supplementation of β-alanine and confirmation through cAMP-PKA and apoptosis pathways in mice. eFood 2 (4), 185–192.

Mallat, Z., Tedgui, A., 2000. Apoptosis in the vasculature: mechanisms and functional importance. Br. J. Pharmacol. 130 (5), 947–962.

Pang, Q., Zhao, Y., Chen, X., Zhao, K., Zhai, Q., Tu, F., 2018. Apigenin protects the brain against ischemia/reperfusion injury via caveolin-1/VEGF *in vitro* and *in vivo*. Oxid. Med. Cell. Longev. 2018.

Plotnikov, A., Zehorai, E., Procaccia, S., Seger, R., 2011. The MAPK cascades: signaling components, nuclear roles and mechanisms of nuclear translocation. Biochim. Biophys. Acta Mol. Cell Res. 1813 (9), 1619–1633.

Qin, W., Ren, B., Wang, S., Liang, S., He, B., Shi, X., Wang, L., Liang, J., Wu, F., 2016. Apigenin and naringenin ameliorate PKCβII-associated endothelial dysfunction via regulating ROS/caspase-3 and NO pathway in endothelial cells exposed to high glucose. Vasc. Pharmacol. 85, 39–49.

Senyildiz, M., Alpertunga, B., Ozden, S., 2017. DNA methylation analysis in rat kidney epithelial cells exposed to 3-MCPD and glycidol. Drug Chem. Toxicol. 40 (4), 432–439.

Sevim, Ç., Özkaraca, M., Kara, M., Ulaş, N., Mendil, A.S., Margina, D., Tsatsakis, A., 2021. Apoptosis is induced by sub-acute exposure to 3-MCPD and glycidol on Wistar Albino rat brain cells. Environ. Toxicol. Pharmacol. 87, 103735.

Sui, X., Kong, N., Ye, L.I., Han, W., Zhou, J., Zhang, Q., He, C., Pan, H., 2014. p38 and JNK MAPK pathways control the balance of apoptosis and autophagy in response to chemotherapeutic agents. Cancer Lett. 344 (2), 174–179.

Wang, J., Liao, Y., Fan, J., Ye, T., Sun, X., Dong, S., 2012. Apigenin inhibits the expression of IL-6, IL-8, and ICAM-1 in DEHP-stimulated human umbilical vein endothelial cells and in vivo. Inflammation 35 (4), 1466–1476.

Wang, R., Tao, M., Zhu, Y., Fan, D., Wang, M., Zhao, Y., 2021a. Puerarin inhibited 3-chloropropane-1, 2-diol fatty acid esters formation by reacting with glycidol and glycidyl esters. Food Chem. 358, 129843.

Wang, Y., Liu, N., Huang, X., Hu, W., Ma, Y., Liang, Y., Xie, W., Tang, M., 2021b. Atmospheric particulate matter impedes autophagic flux by impairing lysosomal milieu and integrity in human umbilical vein endothelial cells (HUVECs). Sci. Total Environ. 761, 143290.

Yamada, T., Egashira, N., Imuta, M., Yano, T., Yamauchi, Y., Watanabe, H., Oishi, R., 2010. Role of oxidative stress in vinorelbine-induced vascular endothelial cell injury. Free Radic. Biol. Med. 48 (1), 120–127.

Yao, Z., Wang, L., Cai, D., Jiang, X., Sun, J., Wang, Y., Bai, W., 2021. Warangalone induces apoptosis in HeLa cells via mitochondria-mediated endogenous pathway. eFood 2 (5), 259–270.

Yu, J., Jiang, Q., Liu, N., Fan, D., Wang, M., Zhao, Y., 2022. Apigenin and apigenin-7, 4′-O-dioctanoate protect against acrolein-aggravated inflammation via inhibiting the activation of NLRP3 inflammasome and HMGB1/MYD88/NF-κB signaling pathway in Human umbilical vein endothelial cells (HUVEC). Food Chem. Toxicol. 168, 113400.

Zhang, H., Liu, J., Qu, D., Wang, L., Wong, C.M., Lau, C.W., Huang, Y., Wang, Y.F., Huang, H., Xia, Y., Xiang, L., Cai, Z., Liu, P., Wei, Y., Yao, X., Ma, R.C.W., Huang, Y., 2018. Serum exosomes mediate delivery of arginase 1 as a novel mechanism for endothelial dysfunction in diabetes. Proc. Natl. Acad. Sci. USA 115 (29), E6927–E6936.

Zhao, Y., Fan, D., Ru, B., Cheng, K.W., Hu, S., Zhang, J., Li, E.T., Wang, M., 2016. 6-C-(E-phenylethenyl) naringenin induces cell growth inhibition and cytoprotective autophagy in colon cancer cells. Eur. J. Cancer 68, 38–50.

Zhao, Y., Fan, D., Zheng, Z.P., Li, E.T., Chen, F., Cheng, K.W., Wang, M., 2017a. 8-C-(E-phenylethenyl) quercetin from onion/beef soup induces autophagic cell death in colon cancer cells through ERK activation. Mol. Nutr. Food Res. 61 (2), 1600437.

Zhao, Y., Li, E.T., Wang, M., 2017b. Alisol B 23-acetate induces autophagic-dependent apoptosis in human colon cancer cells via ROS generation and JNK activation. Oncotarget 8 (41), 70239.

Zhao, Y., Zhang, X., Zhang, N., Zhou, Q., Fan, D., Wang, M., 2022. Lipophilized apigenin derivatives produced during the frying process as novel antioxidants. Food Chem. 379, 132178.

Zhao, Y., Zhou, Y., Wang, M., 2019. Brosimone I, an isoprenoid-substituted flavonoid, induces cell cycle G 1 phase arrest and apoptosis through ROS-dependent endoplasmic reticulum stress in HCT116 human colon cancer cells. Food Funct. 10 (5), 2729–2738.

Zhou, Q., Cheng, K.W., Gong, J., Li, E.T., Wang, M., 2019. Apigenin and its methylglyoxal-adduct inhibit advanced glycation end products-induced oxidative stress and inflammation in endothelial cells. Biochem. Pharmacol. 166, 231–241.